Chem. 226, 497-509.
Hansch, C. (1969), *Acc. Chem. Res. 2,* 232-239.
Harris, E. J. (1972), in Transport and Accumulation in Biological Systems, 3rd ed, Baltimore, Md., University Park Press, pp. 1-34.
Henderson, P. J. F., McGivan, J. D., and Chappell, J. B. (1969), *Biochem. J. 111,* 521-535.
Jilka, R. L., and Martonosi, A. N. (1975), *J. Biol. Chem. 250,* 7511-7524.
Johnson, S. M., and Bangham, A. D. (1969), *Biochim. Biophys. Acta 193,* 82-91.
Krasne, S., Eisenman, G., and Szabo, G. (1971), *Science 174,* 412-415.
Martonosi, A., Donley, J., and Halpin, R. A. (1968), *J. Biol. Chem. 243,* 61-70.
Newman, G. C., and Huang, C. (1975), *Biochemistry 14,* 3363-3370.
Pfeiffer, D. R., and Lardy, H. A. (1976), *Biochemistry 15,* 935-943.
Pfeiffer, D. R., Reed, P. W., and Lardy, H. A. (1974), *Biochemistry 13,* 4007-4014.
Pressman, B. C. (1970), *Antimicrob. Agents Chemother. 1969,* 28.
Pressman, B. C. (1973), *Fed. Proc., Fed. Am. Soc. Exp. Biol. 32,* 1698-1703.
Reed, P. W., and Lardy, H. A. (1972), *J. Biol. Chem. 247,* 6970-6977.
Scarpa, A., and Inesi, G. (1972), *FEBS Lett. 22,* 273-276.
Schreier-Muccillo, S., Marsh, D., Dugas, H., Schneider, H., and Smith, I. C. P. (1973), *Chem. Phys. Lipids 10,* 11-27.
Szabo, G. (1974), *Nature (London) 252,* 47-79.
Szabo, G., Eisenman, G., McLaughlin, S. G. A., and Krasne, S. (1972), *Ann. N.Y. Acad. Sci. 195,* 273-290.
Taussky, H. H., and Shorr, E. (1953), *J. Biol. Chem. 202,* 675-685.
Waku, K., Uda, Y., and Nakazawa, Y. (1971), *J. Biochem. (Tokyo) 69,* 483-491.
Wong, D. T., Wilkinson, J. R., Hamill, R. L., and Horng, J-S. (1973), *Arch. Biochem. Biophys. 156,* 578-585.
Wun, T-C., Bittman, R., and Borowitz, I. J. (1977), *Biochemistry 16* (preceding paper in this issue).

High-Resolution Nuclear Magnetic Resonance Determination of Transfer RNA Tertiary Base Pairs in Solution. 1. Species Containing a Small Variable Loop†

Brian R. Reid,* N. Susan Ribeiro, Lillian McCollum, Joseph Abbate, and Ralph E. Hurd

ABSTRACT: Eight class I tRNA species have been purified to homogeneity and their proton nuclear magnetic resonance (NMR) spectra in the low-field region (−11 to −15 ppm) have been studied at 360 MHz. The low-field spectra contain only one low-field resonance from each base pair (the ring NH hydrogen bond) and hence directly monitor the number of long-lived secondary and tertiary base pairs in solution. The tRNA species were chosen on the basis of their sequence homology with yeast phenylalanine tRNA in the regions which form tertiary base pairs in the crystal structure of this tRNA. All of the spectra show 26 or 27 low-field resonances approximately 7 of which are derived from tertiary base pairs. These results are contrary to previous claims that the NMR spectra indicate the presence of resonances from secondary base pairs only, as well as more recent claims of only 1-3 tertiary resonances, but are in good agreement with the number of tertiary base pairs expected in solution based on the crystal structure. The tertiary base pair resonances are stable up to at least 46 °C. Removal of magnesium ions causes structural changes in the tRNA but does not result in the loss of any secondary or tertiary base pairs.

Early NMR[1] studies on model base pairs in aprotic solvents revealed that the hydrogen bonded ring NH resonance is greatly deshielded and occurs in the extreme low-field end of the proton spectrum (Katz and Penman, 1966). The pioneering studies of Kearns et al. (1971a,b) showed that, in solutions of tRNA, the solvent-exchangeable base pair ring NH hydrogen bonds were sufficiently long-lived to generate discrete low-field (−11 ppm to −15 ppm) resonances even in H_2O solvents. Since each base pair contains only one ring NH hydrogen bond, low-field NMR spectroscopy appeared an ideal method to study the number of tRNA base pairs in solution under a variety of conditions. During the ensuing 5 years, the extent of base pairing in several class I tRNAs has been studied by this technique; these tRNA species have a four base-paired DHU helix, a five nucleotide variable loop containing m^7G, and contain a total of 19 or 20 secondary base pairs in their cloverleaf structure.

By far the most studied class I D4V5 tRNA species has been yeast $tRNA^{Phe}$, because of its ease of isolation. Over the last

† From the Biochemistry Department, University of California, Riverside, California 92502. *Received December 20, 1976.* This work was supported by grants from the National Science Foundation (PCM73-01675), the American Cancer Society (NP-191), and the National Cancer Institute, Department of Health, Education and Welfare (CA11697). The Stanford Magnetic Resonance Laboratory Bruker HXS 360 spectrometer, Stanford, California, was established with a National Science Foundation grant and a United States Public Health Service Biotechnology Resources grant.

[1] Abbreviations used are: DHU, dihydrouridine; rT, ribothymidine; m^7G, N^7-methylguanosine; Ψ, pseudouridine; tRNA, transfer ribonucleic acid; EDTA, ethylenediaminetetraacetic acid; NMR, nuclear magnetic resonance; DEAE, diethylaminoethyl; BD, benzoylated diethylaminoethyl; UV, ultraviolet; CW, continuous wave; DSS, 2,2-dimethylsilapentane-5-sulfonate.

few years several NMR studies on yeast $tRNA^{Phe}$ by Kearns and co-workers have claimed the presence of only 19 low-field base pair resonances (Kearns et al., 1973a), which was subsequently revised to 19.7 resonances (Kearns et al., 1973b; Jones and Kearns, 1974, 1975; Wong et al., 1975a). Yeast $tRNA^{Phe}$ contains 20 secondary Watson–Crick base pairs and 1 GU pair; the absence of additional tertiary resonances and the lack of one secondary base pair (assigned to AU5) in the 19-resonance spectrum have been discussed in a review by Kearns and Shulman (1974).

Similarly, *E. coli* $tRNA^{fMet}$ has been studied by low-field NMR spectroscopy and interpreted to contain 19 base pair resonances (Crothers et al., 1974) by one group and 22 base pair resonances by others (Wong et al., 1975c). Another class I tRNA, namely, *E. coli* $tRNA^{Trp}$, was studied by NMR and found to contain 21.6 low-field base-pair (Jones et al., 1976). The conclusion from this series of studies was that these tRNAs contain between −1 and +2 additional base pairs in solution above those expected from the secondary structure. Since the tertiary folding of yeast $tRNA^{Phe}$ in the crystal structure reveals 7 tertiary base pairs involving ring NH hydrogen bonds (Quigley et al., 1975; Ladner et al., 1975), it appeared that the majority of the tertiary crystallographic interactions were not observable in the NMR spectrum, due either to rapid solvent exchange of the tertiary base pairs or to the solution structure differing from the crystal structure.

In 1975 we carried out a NMR study on *E. coli* $tRNA^{Val}_1$ which contains 20 secondary base pairs and exhibits a well-resolved low-field spectrum. The spectrum was found to contain, by two independent methods, 26 ± 1 low-field base-pair resonances, reflecting 6 ± 1 stable tertiary base pairs involving ring NH hydrogen bonds (Reid and Robillard, 1975); the origin of these 6–7 tertiary resonances was discussed with respect to the tRNA crystal structure. Wong et al. (1975b) and Bolton and Kearns (1976) have disagreed with our interpretation of the *E. coli* $tRNA^{Val}_1$ spectrum claiming from their own studies on this tRNA that the spectrum contains 20 base-pair resonances in the absence of magnesium and 23 resonances in 15 mM magnesium. More recently, Bolton et al. (1976) have reported a comparative NMR study on the number of solution base pairs in several class I tRNAs; the species studied were yeast $tRNA^{Phe}$ (19.6–22.2 resonances), *E. coli* $tRNA^{fMet}$ (23 resonances), *E. coli* $tRNA^{Glu}_{1,2}$ (21.5 resonances), *E. coli* $tRNA^{Val}_1$ (23 resonances), *E. coli* $tRNA^{Asp}$ (20.2 resonances), and *E. coli* $tRNA^{Trp}$ (19 resonances in 3 mM magnesium, 22 resonances in 40 mM magnesium). These values are somewhat higher than those reported earlier and they attribute the discrepancy in part to insufficient magnesium in the earlier samples; however, even in the presence of excess magnesium, the number of additional tertiary resonances was claimed to be less than half of the 7 tertiary ring NH base pairs seen in the crystal structure of yeast $tRNA^{Phe}$.

We have recently completed a high-resolution NMR study of 14 homogeneous class I tRNA species. The purpose of this communication is to report on the number of stable secondary and tertiary base pairs in solution and the effect of magnesium deprivation on tertiary base pairing in class I tRNAs.

Materials and Methods

A combination of three, and where necessary four, standard chromatographic techniques was used to purify the various tRNA species from unfractionated tRNA. These are: (1) chromatography on benzoylated DEAE-cellulose as described by Gillam et al. (1967); (2) chromatography on DEAE-Sephadex as described by Nishimura (1971) using 6-L gradients from 0.4 M to 0.5 M NaCl; (3) reverse gradient Sepharose 4B chromatography as described by Holmes et al. (1975); and (4) RPC5 chromatography as described by Pearson et al. (1971) using 0.4 M to 0.9 M NaCl gradients at pH 4.5 in 0.01 M acetate buffer.

E. coli $tRNA^{Val}_1$. The $tRNA^{Val}_1$ species was resolved from the later-eluting (1.02 M NaCl) Val-2A and Val-2B species on BD-cellulose chromatography. The early-eluting (0.73 M NaCl) 12-fold purified Val-1 tRNA was purified to homogeneity by DEAE-Sephadex chromatography. The final material accepted 1860 pmol of valine per A_{260} when aminoacylated with pure valyl-tRNA synthetase.

E. coli $tRNA^{Arg}_1$. The second half of the broad major BD-cellulose arginine tRNA peak (0.9 M NaCl) was further purified by DEAE-Sephadex chromatography. This material was then purified to homogeneity by Sepharose 4B chromatography followed by RPC5 chromatography. The final material accepted 1600 pmol of arginine per A_{260} when aminoacylated with partially purified arginyl-tRNA synthetase.

E. coli $tRNA^{His}$. The broad histidine tRNA peak eluting from BD-cellulose at 0.88 M NaCl was further purified by DEAE-Sephadex chromatography followed by Sepharose 4B chromatography which resolved a major early-eluting histidine tRNA from a minor later-eluting histidine peak. The earlier major species was purified to homogeneity by RPC5 chromatography. The final material accepted 1650 pmol of histidine per A_{260} when aminoacylated with partially purified histidyl-tRNA synthetase.

E. coli $tRNA^{fMet}$ *and* $tRNA^{mMet}$. The early eluting (0.73 M NaCl) fMet species was well-resolved from the later-eluting (0.87 M NaCl) mMet species on BD-cellulose chromatography. Each methionine fraction was separately purified to homogeneity by DEAE-Sephadex chromatography. The final fMet preparation and the final mMet preparation accepted 1950 and 1840 pmol of methionine, respectively, per A_{260} when aminoacylated with 50% pure methionyl-tRNA synthetase.

Yeast $tRNA^{Phe}$. This material was purified to 95% homogeneity as described previously (Schmidt et al., 1970).

E. coli $tRNA^{Gly}_3$. The BD-cellulose glycine profile revealed two early-eluting minor glycine peaks (Gly-1, Gly-2) and a later-eluting (0.86 M NaCl) major peak of Gly-3 tRNA. This latter material was further purified by DEAE-Sephadex, Sepharose 4B, and RPC5 chromatography. The final preparation accepted 1580 pmol of glycine per A_{260} when aminoacylated with crude glycyl-tRNA synthetase.

E. coli $tRNA^{Lys}$. A double peak of lysine activity eluting at 0.8 M NaCl was observed on BD-cellulose chromatography. The slightly earlier of the two lysine peaks was further purified by DEAE-Sephadex and Sepharose 4B chromatography. The final material accepted 1400 mol of lysine per A_{260} when aminoacylated with crude lysyl-tRNA synthetase.

E. coli $tRNA^{Lys}$. A double peak of lysine activity eluting at 0.8 NaCl was observed on BD-cellulose chromatography. The slightly earlier of the two lysine peaks was further purified by DEAE-Sephadex and Sepharose 4B chromatography. The final material accepted 1400 pmol of lysine per A_{260} when aminoacylated with crude lysyl-tRNA synthetase.

Identification of tRNAs and Isoaccepting Species. In all cases the isolated tRNA species were subjected to RNase T1 fingerprinting and shown to have the same fingerprint as that published in the course of sequencing these tRNAs. Two-dimensional fingerprints were carried out according to Barrell (1971) on 30 A_{260} units of material using Whatman 3MM paper instead of cellulose acetate strips in the first dimension, and also by two-dimensional TLC separation on 2.5 A_{260} units

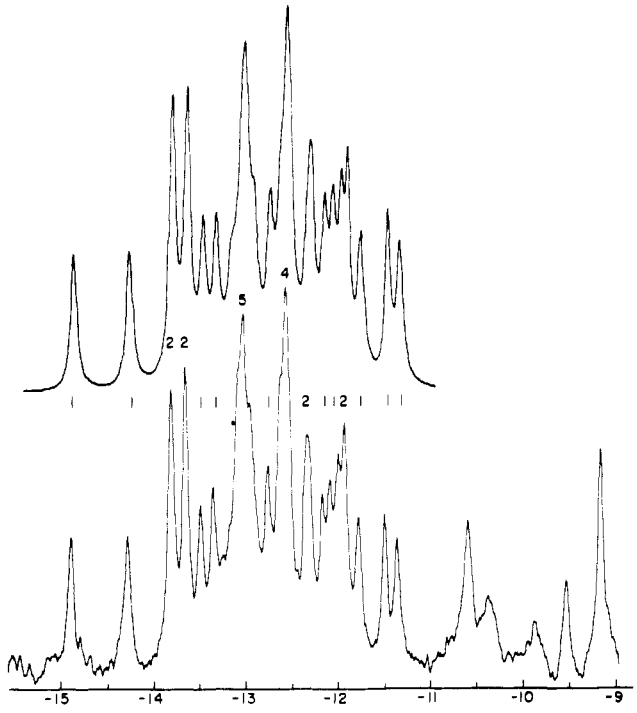

FIGURE 1: The 360-MHz NMR spectrum of *E. coli* $tRNA^{Val}_1$ (1.1 mM) at 39 °C; solvent 10 mM sodium cacodylate–100 mM NaCl–15 mM $MgCl_2$ (pH 7.0). The experimental spectrum (lower) was obtained under correlation sweep conditions as described in Materials and Methods; the intensity is shown at the top of each peak. The simulated spectrum (upper trace) contains 27 convoluted Lorentzian lines of line width 30 Hz.

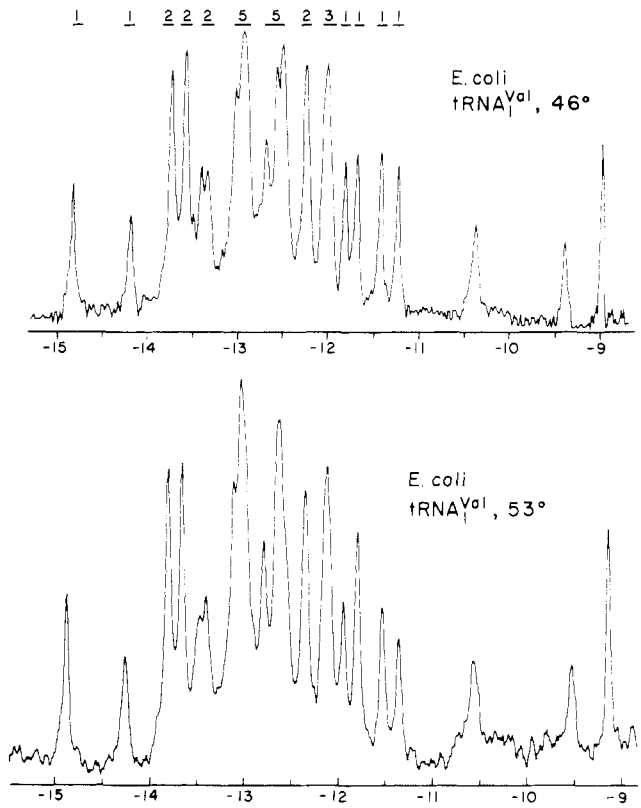

FIGURE 2: The 360-MHz NMR spectrum of *E. coli* $tRNA^{Val}_1$ at 46 °C (upper) and 53 °C (lower). The material is the same sample in the same solvent which produced the 39 °C spectrum in Figure 1. Signal-averaging correlation spectroscopy conditions are the same as in Figure 1 and described in Materials and Methods.

of material according to Schoemaker and Schimmel (1974). Spots were visualized with an UV lamp. Authentic fingerprints for identification of the *E. coli* tRNA species were taken from the following references: Val-1, Harada et al. (1969); Arg-1, Murao et al. (1972) and Chakraburrty (1975) (although the latter sequence is referred to as $tRNA^{Arg}_2$, it differs from the former sequence in only a single nucleotide and a single modification); His, Singer and Smith (1972); Met, Cory and Marcker (1970); fMet, Dube et al. (1969); Gly-3, Squires and Carbon (1971); Lys, Chakraburrty et al. (1975).

NMR Spectra. Lyophilized tRNA samples (5 mg) were dissolved in either a low ionic strength magnesium-deficient buffer (10 mM sodium cacodylate–10 mM EDTA (pH 7.0)) or an intermediate ionic strength magnesium buffer (10 mM sodium cacodylate–0.1 M NaCl–15 mM $MgCl_2$ (pH 7.0)). The samples (0.18 mL containing 1.1 mM tRNA) were transferred to 5 × 8 mm NMR microtubes (Wilmad Glass Co., Buena, N.J.). With two exceptions, the spectra were accumulated using correlation spectroscopy techniques. A sweep width of 2400 Hz, starting 3900-Hz downfield from H_2O, was swept at a rate of 1200 Hz per s. The spectra were correlated after accumulating 600–800 sweeps in a Nicolet signal-averaging computer. For CW spectroscopy 2400 Hz were swept at 200 Hz per s and 500 sweeps were accumulated in a Nicolet signal-averaging computer. The CW spectra were obtained on a Bruker 360-MHz spectrometer at the University of Groningen; the correlation spectra were obtained on the Bruker HXS 360 spectrometer at the Stanford Magnetic Resonance Laboratory, Palo Alto, Calif. Chemical shifts are expressed in ppm from 2,2-dimethylsilapentane-5-sulfonate. Experimentally, the shifts were determined from the H_2O solvent, to which the known chemical shift of water from DSS at the corresponding temperature was then added. The experimental spectra were printed out directly onto 8.5 in. × 11 in. sheets of plain white paper by reducing the x and y axes in the signal-averaging computer.

Integration and Simulation of Spectra. Separate NMR peaks (resolved to at least half-height from adjacent peaks) were initially integrated by measuring the area in cm^2 on the original spectrum. Corroboration of intensities, and precise determination of the component chemical shifts in complex peaks, was obtained by a simulation computer program. Lorentzian lines, with the experimentally observed width at half-height, were convoluted to generate an approximation of the spectrum. The positions of these lines were then adjusted to generate an exact replica of the experimental spectrum. In this way the number of resonances and the chemical shift of each resonance in the low-field spectrum could be determined.

Results

We have previously shown that the nearest neighbor stacking sequence of *E. coli* $tRNA^{Val}_1$ results in a very well-resolved low-field NMR spectrum for this tRNA (Reid et al., 1975; Reid and Robillard, 1975). We have now examined the effects of solvent, temperature, and magnesium deprivation on the spectrum. Figure 1 shows the 360-MHz low-field spectrum of $tRNA^{Val}_1$ at 39 °C in 15 mM $MgCl_2$; the spectrum is virtually identical with our previous 270-MHz spectrum at 35 °C in 15 mM $MgCl_2$ (Reid et al., 1975), except for the increased resolution at 360 MHz and the increased signal-to-noise ratio using correlation spectroscopy. The spectrum contains 17 peaks in the −11 to −15 ppm region and several of these are obviously complex peaks containing multiple resonances. Integration of the complex peaks with respect to

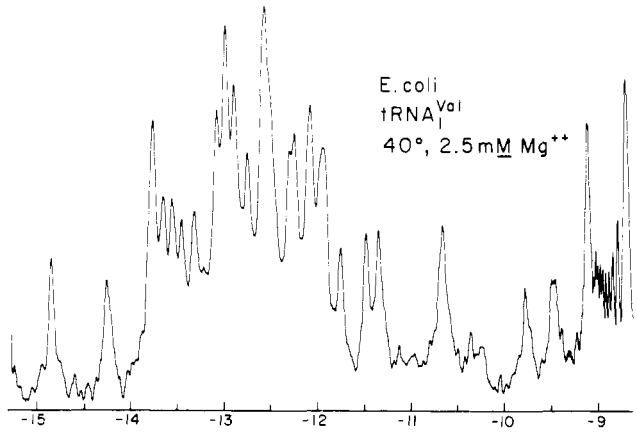

FIGURE 3: The 360-MHz NMR spectrum of *E. coli* tRNA$^{Val}_1$ at 40 °C under limiting magnesium conditions. The tRNA concentration is 1.1 mM and the magnesium concentration is 2.5 mM in a solvent containing 1.7 mM sodium cacodylate and 17 mM NaCl. Correlation spectroscopy conditions as described in Figure 1 and Materials and Methods.

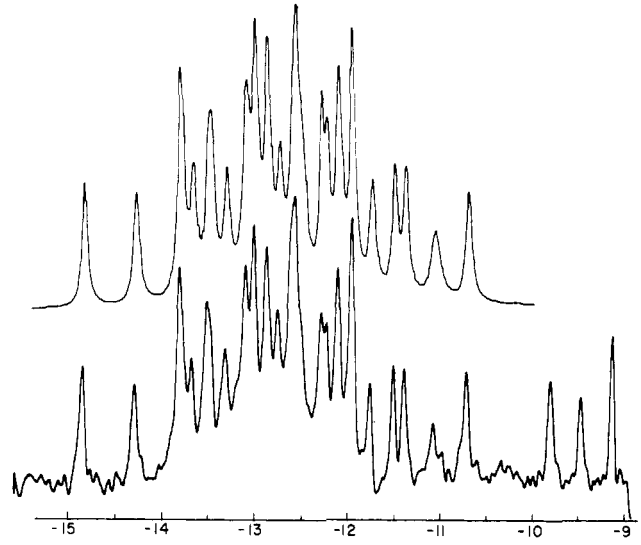

FIGURE 4: The 360-MHz NMR spectrum of *E. coli* tRNA$^{Val}_1$ in the absence of magnesium. An EDTA-dialyzed tRNA sample was dialyzed against distilled water and lyophilized. The sample was then redissolved in 10 mM sodium cacodylate–10 mM sodium EDTA (pH 7.0). The lower trace is the experimental 20-min correlation spectrum. The upper trace is the computer simulation; it contains 27 Lorentzian lines of general line width 28 Hz between −15.0 and −11.3 ppm and two additional lines at −11.07 and −10.71 ppm.

the intensity of the resolved single resonances at −14.9, −14.3, −13.5, −13.4, −11.8, −11.5, and −11.4 ppm leads to the integral (or close to integral) values shown for these peaks; this leads to a total of 27 lowfield resonances (ring NH base pairs) between −11 and −15 ppm. Also shown in Figure 1 is a computer simulation of the spectrum using a set of Lorentzian lines having the experimentally observed single resonance line width; the experimental spectrum can only be simulated with 27 input lines, thus corroborating the intensity obtained by integrating peak areas.

The effect of raising the temperature on the 15 mM $MgCl_2$ sample is shown in Figure 2. At 46 °C the spectrum still contains 27 low-field resonances; however, some interesting minor rearrangements occur which were also noted in our earlier, less resolved, 270-MHz spectra (Reid et al., 1975). The resolved peaks at −13.5 and −13.4 ppm have coalesced somewhat and the seven protons between −12.4 and −11.7 ppm have rearranged from a 2:4:1 grouping to a 2:3:1:1 arrangement. This spectral change is reversible on returning to the lower temperature and we conclude that a structural equilibrium (with rate constants that are slow on the ca. 5-ms NMR time scale) is being perturbed at temperatures around 41 °C, with no loss in tertiary base pairing. As the temperature is raised to 53 °C, the spectrum retains, in a qualitative sense, all the resonances in the characteristic 15-peak pattern of the 46 °C spectrum but there are small losses of intensity in certain peaks, e.g., at −14.3, −13.4, −12.7, −11.9, −11.5, and −11.3 ppm. Hence, although all the secondary and tertiary base pairs are present even at 53 °C, the molecule has begun to undergo local unfolding; the line widths of the decreased resonances indicate that the native structure is in slow exchange with the coil form which shows rapid solvent exchange of the ring NH protons.

Figure 3 shows the tRNA$^{Val}_1$ spectrum at 40 °C in 2.5 mM $MgCl_2$, i.e., a magnesium:tRNA ratio of approximately two. Again we observe some interesting structural rearrangements compared with the 39 °C, 15 mM $MgCl_2$ spectrum. The peak of 2 protons at −13.7 ppm has resolved into two single resonances and the 5 proton peak at −13.0 ppm has begun to resolve. The 7 protons in the −12.4 to −11.7 ppm region show an arrangement which is intermediate between the 39 °C, 15 mM $MgCl_2$ pattern and the 46 °C, 15 mM $MgCl_2$ pattern. The total number of resonances remains 27 under these magnesium-limiting conditions.

To investigate the magnesium effect further, a sample was exhaustively dialyzed against a 50-fold excess of EDTA and then examined in the absence of magnesium in a buffer containing a 9-10-fold excess of EDTA. The spectrum of the completely magnesium-free tRNA at 35 °C is shown in Figure 4. The spectrum is resolved into 19 peaks and several additional rearrangements are observed in the magnesium-free structure. The 4 protons between −13.7 and −13.3 ppm have rearranged from a 2:1:1 pattern into a 1:2:1 arrangement and two of the five protons at −13.0 ppm have moved upfield by ca. 0.15 ppm. The 7 protons between −12.4 and −11.7 ppm are now arranged in a 2:2:2:1 grouping. The computer simulation of the magnesium-free spectrum is also shown in Figure 4. Even in the complete absence of magnesium, the spectrum reveals the presence of 27 long-lived base pairs with a 28th resonance beginning to appear at −11.1 ppm; this last resonance may be a partially exchanging GU ring NH bond or the "protected" anticodon loop U33 ring NH reported by Wong and Kearns (1974).

The three-dimensional folding of yeast tRNA^{Phe} in two different crystal forms is the same, and involves extensive tertiary base pairing between the DHU loop, the rT loop, the variable loop, and the DHU stem (Sussman and Kim, 1976). The positions involved in tertiary interactions show coordinated changes in different tRNAs and this has led to some cogent arguments in favor of a common tRNA folding pattern (Klug et al., 1974; Kim et al., 1974). Hence we decided to study several additional class I tRNAs which, like *E. coli* tRNA$^{Val}_1$, also contain the same DHU stem and the same tertiary folding potential as yeast tRNA^{Phe}. These species are shown in their two-dimensional cloverleaf representations in Figure 5.

The 360-MHz low-field spectrum of *E. coli* tRNA$^{Arg}_1$ at 45 °C in 15 mM $MgCl_2$ is shown in Figure 6. It contains eight well-resolved single proton peaks. Based on these intensities, the four complex peaks contain the intensities indicated. The total number of resonances between −11 and −15 ppm is 27 ± 1.

Figure 7 shows the low-field spectrum of *E. coli* tRNA^{His}

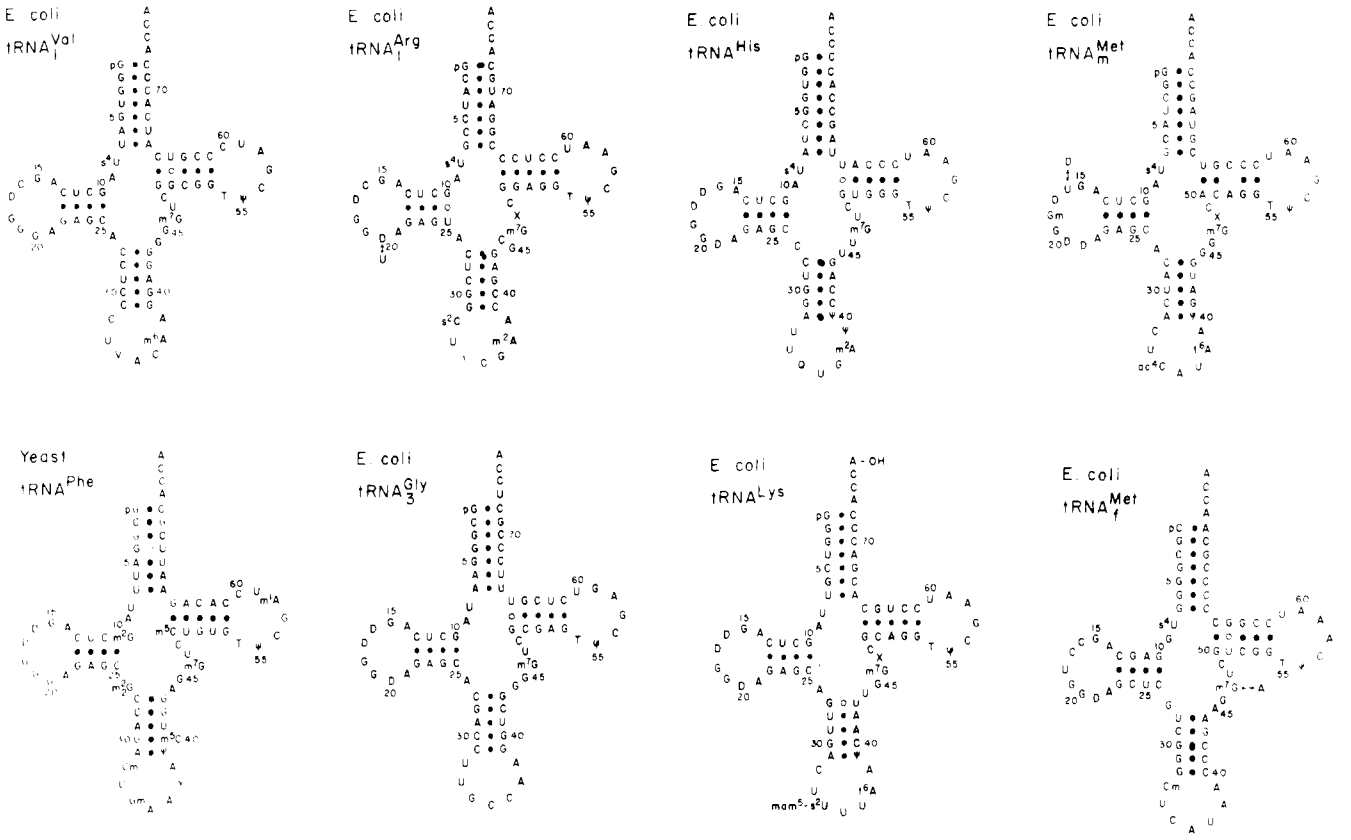

FIGURE 5: Two-dimensional cloverleaf representation of some of the class I D4V5 tRNA species analyzed in this study. The identity of each species was determined by fingerprinting and comparison with the published sequences as described in Materials and Methods. Note the common sequence in the DHU helix followed by residues A and G in the DHU loop, and also the presence of m^7G as the third residue of the five nucleotide variable loop.

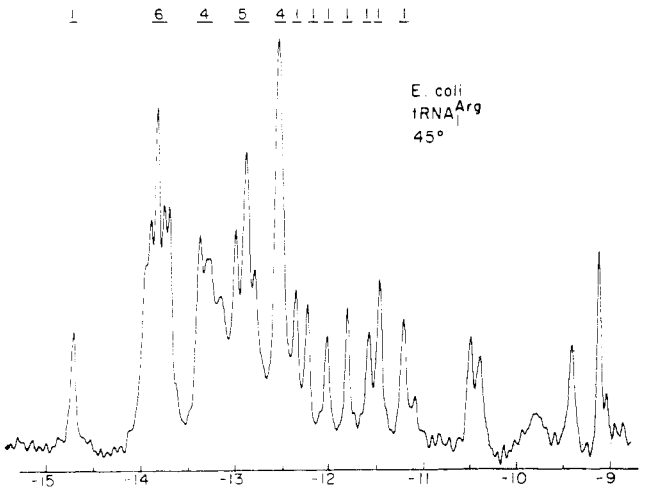

FIGURE 6: The 360-MHz NMR spectrum of *E. coli* tRNA$^{Arg}_1$ at 46 °C in 15 mM $MgCl_2$. Solvent conditions and tRNA concentration as in Figure 1.

at 45 °C in 15 mM $MgCl_2$. The spectrum contains several resolved single proton resonances and integrates to a total of 28 ± 1 base pairs. This is verified by the computer simulation using the experimentally observed line width; the simulated spectrum shown in Figure 7 required 28 Lorentzian lines in the computer input.

The spectrum of *E. coli* tRNA^{mMet} at 45 °C in 15 mM $MgCl_2$ is shown in Figure 8 together with the computer simulation. The spectrum integration indicated 27 ± 1 resonances

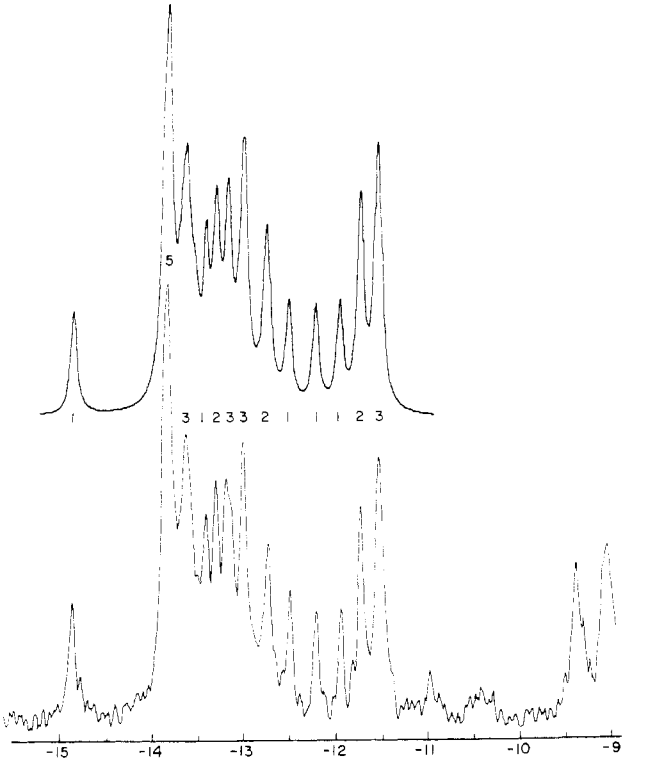

FIGURE 7: The 360-MHz NMR spectrum of *E. coli* tRNA^{His} at 45 °C in 15 mM $MgCl_2$. Correlation parameters and solvent conditions as described in Figure 1 and Materials and Methods. The intensity is indicated on each peak. The upper trace is a computer simulation using 28 Lorentzian lines of general line width 30 Hz.

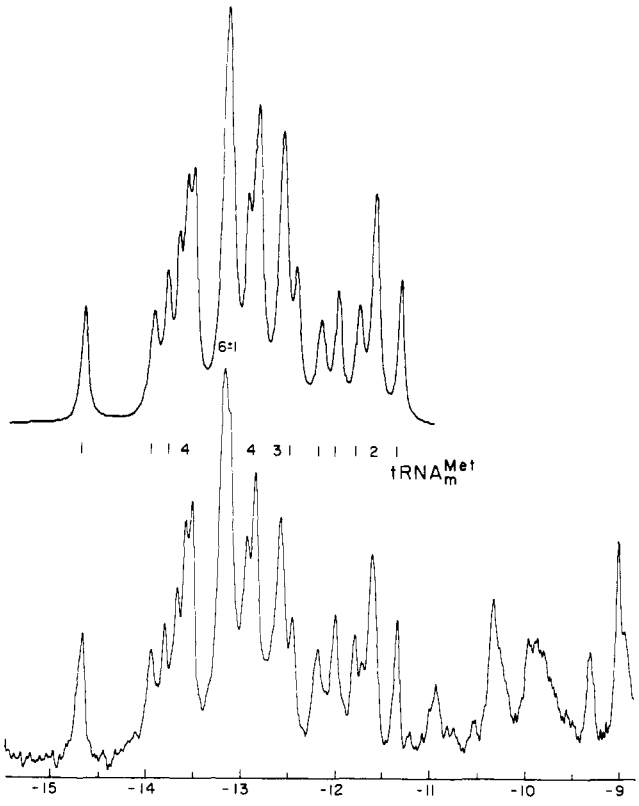

FIGURE 8: The 360-MHz NMR spectrum of *E. coli* $tRNA^{mMet}$ at 45 °C in 10 mM sodium cacodylate–100 mM NaCl–15 mM $MgCl_2$ (pH 7.0). The intensity is indicated on each peak. The spectrum could be simulated with either 26 or 27 lines of 30-Hz line width; the upper trace is a simulation with 26 lines and the simulated intensity is slightly less than the experimental intensity at −13.2 ppm.

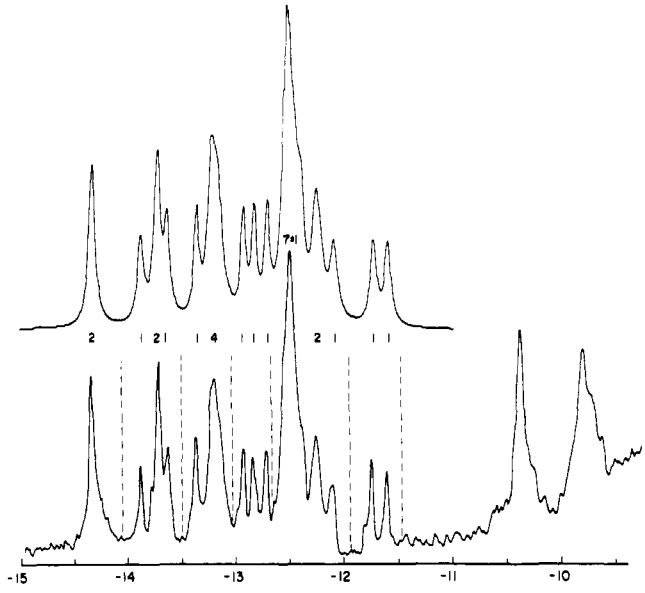

FIGURE 9: The 360-MHz spectrum of yeast $tRNA^{Phe}$ in the absence of magnesium. A water-dialyzed, lyophilized sample was redissolved to 1.1 mM concentration in 10 mM sodium cacodylate–10 mM EDTA (pH 7.0). Peak intensities are indicated on the experimental spectrum (lower). The computer-simulated spectrum (upper) contains 26 Lorentzian lines of 25-Hz general line width.

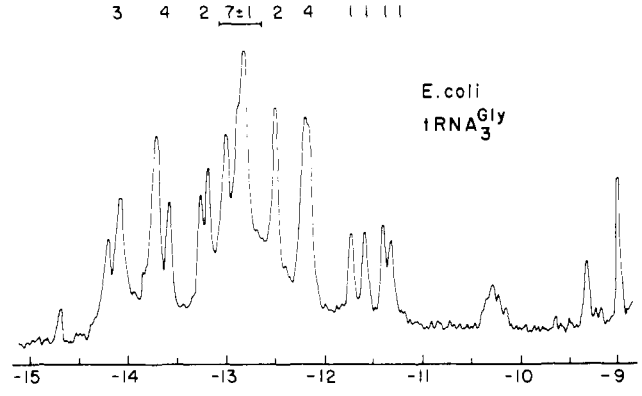

FIGURE 10: The 360-MHz NMR spectrum of *E. coli* $tRNA^{Gly}_3$ at 45 °C in 15 mM $MgCl_2$. Conditions are as described in Figure 1 and peak intensities are indicated on the spectrum. The purified material exhibited approximately one-third of the extinction at 340 nm expected for a tRNA with a single residue of 4-thiouridine; we presume the material was incompletely thiolated at position 8, thus explaining the small peak at −14.75 ppm.

and acceptable computer simulations required either 26 or 27 input lines. The simulation shown in Figure 8 contains 26 resonances; however, the simulated peak at −13.2 ppm contains only 5 lines and is somewhat lower in intensity than the experimental peak.

Figure 9 shows the low-field spectrum of yeast $tRNA^{Phe}$ at 360 MHz. The spectrum shown is of a magnesium-free sample dissolved in a buffer containing a tenfold molar excess of EDTA; the spectrum shows greater resolution in this solvent than in magnesium-containing buffers and our data with $tRNA^{Val}_1$ indicate that the total number of low-field resonances does not change under these conditions. Although the spectrum is inherently less well-resolved than other tRNA spectra, there are nevertheless several resolved peaks of single proton intensity. Based on these intensities, the spectrum reflects the presence of a total of 26 ± 1 secondary and tertiary base pairs which generate a ring NH resonance between −11 and −15 ppm. The computer simulation, using the experimentally determined line width, corroborates this value.

The 360-MHz low-field spectrum of *E. coli* $tRNA^{Gly}_3$ at 45 °C in 15 mM $MgCl_2$ is shown in Figure 10. The spectrum is resolved into 14 peaks; integration of each peak leads to an intensity of 26 ± 1 resonances between −11 and −15 ppm.

Figure 11 shows the low-field spectrum of *E. coli* $tRNA^{Lys}$ at 45 °C in 15 mM $MgCl_2$. The spectrum contains 17 peaks between −11 and −15 ppm and integrates to a total intensity of 26 ± 1 protons.

Although *E. coli* $tRNA^{fMet}$ does not contain the same sequence as yeast $tRNA^{Phe}$ in its DHU stem, we nevertheless decided to purify this tRNA and study its low-field spectrum during this series of experiments. The NMR spectrum of this tRNA has been studied in detail by several different groups; the total number of low-field base-pair proton resonances has been variously claimed to be 19 (Crothers et al., 1974), or 22 (Wong et al., 1975c), or 27 (Daniel and Cohn, 1975). The $tRNA^{fMet}$ 360-MHz spectrum at 45 °C in 15 mM $MgCl_2$ is shown in Figure 12. There are 16 peaks between −11 and −15 ppm and the spectrum contains several resolved single proton resonances; integration of the complex peaks leads to a total intensity of 28 ± 2 protons.

Discussion

The total number of low-field base-pair proton resonances, together with the number of secondary cloverleaf base pairs, for several class I tRNAs is presented in Table I. In all cases the spectra contain ca. 27 resonances of which approximately

TABLE I: The Number of Secondary and Tertiary Base Pairs Detectable in the Low-Field NMR Spectra of Several tRNA Species under Different Solvent Conditions and Temperatures.

tRNA Species	Conditions	Temp (°C)	No. of Low-Field Base-Pair Resonances	Secondary Base Pairs	No. of Tertiary Base Pairs
E. coli $tRNA^{Val}_1$	15 mM $MgCl_2$	39	27	20	7
E. coli $tRNA^{Val}_1$	15 mM $MgCl_2$	46	27 ± 1	20	7 ± 1
E. coli $tRNA^{Val}_1$	2.5 mM $MgCl_2$	40	27 ± 1	20	7 ± 1
E. coli $tRNA^{Val}_1$	No Mg^{2+}; 10 mM EDTA	35	27 ± 1	20	7 ± 1
E. coli $tRNA^{Arg}_1$	15 mM $MgCl_2$	45	27 ± 1	20	7 ± 1
E. coli $tRNA^{His}$	15 mM $MgCl_2$	45	28 ± 1	21	7 ± 1
E. coli $tRNA^{mMet}$	15 mM $MgCl_2$	45	27 ± 1	20	7 ± 1
Yeast $tRNA^{Phe}$	No Mg^{2+}; 10 mM EDTA	35	26 ± 1	20	6 ± 1
E. coli $tRNA^{Gly}_3$	15 mM $MgCl_2$	45	26 ± 1	20	6 ± 1
E. coli $tRNA^{Lys}$	15 mM $MgCl_2$	45	26 ± 1	20	6 ± 1
E. coli $tRNA^{fMet}$	15 mM MgC_2	45	28 ± 2	19	9 ± 2

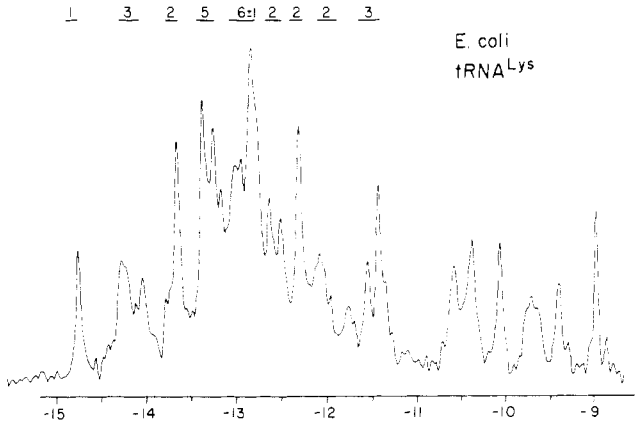

FIGURE 11: The 360-MHz NMR spectrum of *E. coli* $tRNA^{Lys}$ at 45 °C in 15 mM $MgCl_2$. Conditions are as described in Figure 1 and peak intensities are indicated on the spectrum.

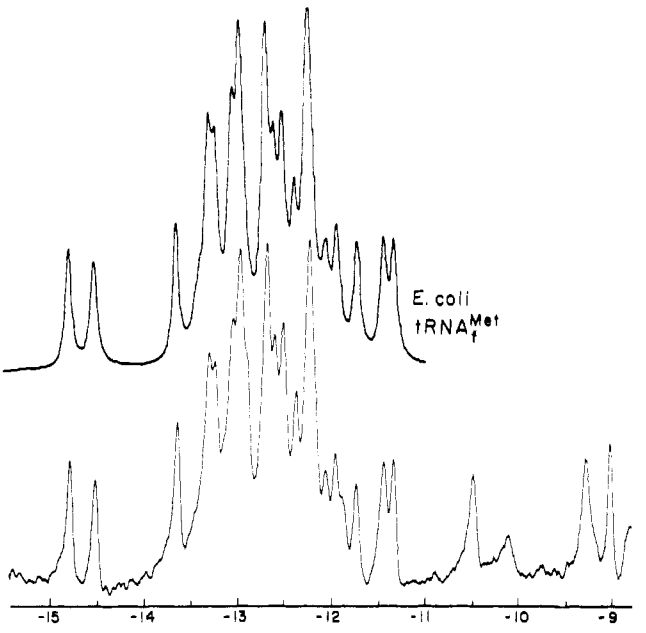

FIGURE 12: The 360-MHz NMR spectrum of *E. coli* $tRNA^{fMet}$ at 45 °C in 15 mM $MgCl_2$. Conditions as described in Figure 1. Integration of the peaks revealed a total of 28 ± 2 resonances. The computer simulation (upper trace) contained 28 Lorentzian lines of general line width 30 Hz.

7 must be derived from tertiary base-pair interactions involving ring NH hydrogen bonds. In addition to the examples shown here, we have also studied several other class I tRNAs, including yeast $tRNA^{Trp}$, *E. coli* $tRNA^{Ala}_1$, $tRNA^{Thr}_1$, $tRNA^{Gly}_2$, $tRNA^{Val}_{2A}$, $tRNA^{Val}_{2B}$, and $tRNA^{Phe}$ and obtained the same result.

All of the tRNAs presented here, with the exception of $tRNA^{fMet}$, contain the yeast $tRNA^{Phe}$ base pair sequence GC-CG-UA-CG in their DHU stem and contain the same "tertiary folding potential" as does yeast $tRNA^{Phe}$ (Kim et al., 1974; Klug et al., 1974). The tertiary base pairs involving ring NH hydrogen bonds in the yeast $tRNA^{Phe}$ crystal structure are U8-A14, G15-C48, G18-Ψ55, G19-C56, m^7G46-G22, T54-m^1A58, and m^2_2G26-A44 (Sussman and Kim, 1976). There is an eighth tertiary base-base interaction involving A9-A23 which involves amino group hydrogen bonds only; the amino group hydrogen bonds do not generate low-field resonances (Katz and Penman, 1966). In all the tRNAs presented in this study, the same "tertiary nucleotides" are present in the corresponding positions in the sequence with the exception of the Pu26-Pu44 interaction which in some cases is A26-G44 instead of G26-A44, and in other cases does not involve two purines. We conclude that these crystallographically determined tertiary ring NH interactions are responsible for the extra resonances in the low-field spectrum over and above the expected 20 resonances from secondary structure. The excellent agreement between the crystal structure and the number of extra resonances in the low-field NMR spectra can be construed as evidence that the crystal structure and the solution structure are the same; however, caution should be exercised on this point since the structural changes observed by varying either temperature or divalent cation concentration may well indicate an equilibrium between related structures in solution. Further evidence for more than one structure in solution comes from slow exchange splitting of certain high-field methyl resonances (Hurd and Reid, unpublished data).

Although yeast $tRNA^{Phe}$ is the only species for which a three-dimensional crystal structure is available, the fact that all the class I tRNAs we have studied show ca. 7 tertiary ring NH base pairs can be taken as strong evidence in support of the previously proposed general folding scheme for these tRNAs (Kim et al., 1974; Klug et al., 1974).

Several of the tRNA species which we have investigated have also been studied by low-field NMR spectroscopy by others, but our conclusions concerning the number of tertiary resonances are quite different. For instance, the low-field spectrum of *E. coli* $tRNA^{Val}_1$ has been reported to contain 20

resonances in the absence of magnesium and 23 resonances in the presence of magnesium (Bolton and Kearns, 1976: Bolton et al., 1976). The low-field spectrum of *E. coli* $tRNA^{fMet}$ has been interpreted to contain 19 protons (Crothers et al., 1974), 22 protons (Wong et al., 1975c), 23 protons (Bolton et al., 1976), or 27 protons (Daniel and Cohn, 1975); our data on this tRNA agree only with the latter group. The low-field spectrum of yeast $tRNA^{Phe}$ has been variously interpreted to contain either zero (Jones and Kearns, 1975; Wong et al., 1975a) or two (Bolton et al., 1976; Kearns, 1976) tertiary resonances. All of the above values, with the exception of the Daniel and Cohn study on $tRNA^{fMet}$, are well below the number of tertiary base pairs which we have observed in the present study.

The discrepancy between their earlier integration and their more recent claims of two to three tertiary resonances has been attributed by Bolton et al. (1976) partly to "lack of magnesium" and partly to the "less accurate integration methods used"; however, the earlier spectra in question were obtained in the presence of eight- to tenfold molar excess of free magnesium. Furthermore, we have shown that limiting magnesium conditions, or even completely magnesium-free conditions in which the dialyzed tRNA sample is dissolved at 1 mM concentration in 10 mM sodium cacodylate containing 10 mM sodium EDTA, do not change the total number of base pairs detected by low-field NMR spectroscopy. The slightly higher, but still low, new values reported by these workers result from a new intensity calibration method based on the total low-field intensity compared with the area of the upfield aromatic peak (Bolton and Kearns, 1976; Bolton et al., 1976; Kearns, 1976). We have pointed out the errors in the assumptions used in this method of calibrating poorly resolved spectra (Reid, 1976). We are at a loss to explain why their spectra show such poor resolution that integration of individual peaks is not possible. The earlier integration of the yeast $tRNA^{Phe}$ spectrum used internal calibration with the complex peak at -13.75 ppm assumed to have a reference intensity of 3.00 protons (Jones and Kearns, 1975; Wong et al., 1975a; Kearns, 1976). We have resolved this peak into three peaks in EDTA buffers; in the presence of CsCl the resolution is improved further and reveals three separated peaks of intensities 1:2:1 (Reid and Robillard, unpublished data). Hence there are 4 protons in the "3 proton reference peak" thus explaining the low values reported by this group which are consistently 75% of the correct value.

It is obvious that extremely well-resolved spectra are essential in answering the integration question since this permits independent integration of discrete individual peaks rather than having to integrate the whole unresolved low-field region of the spectrum. The maximum resolution of a class I tRNA spectrum we have obtained is unfortunately only 19 peaks in the case of *E. coli* $tRNA^{Val}_1$ in the absence of magnesium. Under conditions of no magnesium, the *E. coli* $tRNA^{Val}_1$ spectrum has been reported to contain 20 protons (Bolton and Kearns, 1976). If this were the case, then the 19 peak spectrum we obtain must contain one peak of two protons and 18 single proton peaks; we submit that this is not the case (see Figure 4).

An interesting aspect of the results we have presented is the observation that magnesium-limiting conditions and magnesium-deficient conditions lead to structural changes in tRNA as evidenced by shifting of resonances. These effects, especially those observed between 15 mM $MgCl_2$ and 2.5 mM $MgCl_2$, may reflect physiologically important structural equilibria. We note that a major conformational rearrangement of tRNA under similar magnesium-limiting conditions has been observed by laser light scattering (Olson et al., 1976). Relatively few tRNA NMR magnesium titration studies have been carried out in the past. In an earlier collaborative project, we studied the low-field NMR spectrum of yeast $tRNA^{Phe}$, and other tRNAs, in buffered solutions containing 10 mM $MgCl_2$ and 0.1 M NaCl (Shulman et al., 1973). Jones and Kearns (1974) have studied the low-field NMR spectrum of yeast $tRNA^{Phe}$ in solutions containing only 10 mM sodium cacodylate and 0.1 M NaCl. The two spectra are surprisingly similar; careful comparison reveals no changes in any resonances (or even in the random baseline noise!). Our own spectra of yeast $tRNA^{Phe}$ and *E. coli* $tRNA^{Val}_1$ do reveal characteristic shifts of certain resonances in the absence of magnesium; since the majority of the spectrum does not change, it is tempting to speculate that these shifts may be diagnostic of tertiary resonances. We are currently involved in experimentally identifying which resonances are derived from tertiary base pairs and attempting to specifically assign the tertiary resonances to the various crystallographically determined ring NH interactions. The theoretically computed NMR spectrum of the crystal structure of yeast $tRNA^{Phe}$ has been calculated and comparison with our experimental spectrum has led Robillard et al. (1976) to propose some tertiary assignments. With two exceptions, these predictions agree reasonably well with our own preliminary experimental tertiary assignments from comparative studies and chemical modification (Hurd, Abbate, and Reid, to be published).

Acknowledgments

Two of the spectra were obtained in the continuous wave mode on a Bruker 360-MHz spectrometer at the University of Groningen; Ralph E. Hurd and Brian R. Reid thank the Netherlands Z.W.O. and Dr. G. T. Robillard for the use of this facility and for hospitality in Groningen. The remaining spectra were obtained by correlation spectroscopy on the Stanford Magnetic Resonance Laboratory Bruker HXS 360 spectrometer, Stanford, California. The authors gratefully acknowledge Dr. W. W. Conover and Dr. S. L. Patt of the SMRL for their excellent assistance and patience in teaching us how to obtain correlation spectra.

References

Barrell, B. G. (1974), *Proced. Nucleic Acid Res. 2,* 751–779.

Bolton, P. H., and Kearns, D. R. (1976), *Nature (London) 262,* 423–424.

Bolton, P. H., Jones, C. R., Bastedo-Lerner, D., Wong, K. L., and Kearns, D. R. (1976), *Biochemistry 15,* 4370–4377.

Chakraburrty, K. (1975), *Nucleic Acids Res. 2,* 1787–1792.

Chakraburrty, K., Steinschneider, A., Case, R. V., and Mehler, A. H. (1975), *Nucleic Acids Res. 2,* 2069–2075.

Cory, S., and Marcker, K. A. (1970), *Eur. J. Biochem. 12,* 177–194.

Crothers, D. M., Cole, P. E., Hilbers, C. W., and Shulman, R. G. (1974), *J. Mol. Biol. 87,* 63–88.

Daniel, W. E., and Cohn, M. (1975), *Proc. Natl. Acad. Sci. U.S.A. 72,* 2582–2586.

Dube, S. K., Marcker, K. A., Clark, B. F. C., and Cory, S. (1969), *Eur. J. Biochem. 8,* 244–255.

Gillam, I., Millward, S., Blew, D., Von Tigerstrom, M., Wimmer, E., and Tener, G. M. (1967), *Biochemistry 6,* 3043–3056.

Harada, F., Kimura, F., and Nishimura, S. (1969), *Biochim. Biophys. Acta 195,* 590–592.

Holmes, W. M., Hurd, R. E., Reid, B. R., Rimerman, R. A.,

and Hatfield, G. W. (1975), *Proc. Natl. Acad. Sci. U.S.A. 72,* 1068–1071.
Jones, C. R., and Kearns, D. R. (1974), *Proc. Natl. Acad. Sci. U.S.A. 71,* 4237–4240.
Jones, C. R., and Kearns, D. R. (1975), *Biochemistry 14,* 2660–2665.
Jones, C. R., Kearns, D. R., and Muench, K. (1976), *J. Mol. Biol. 103,* 747–764.
Katz, L., and Penman, S. (1966), *J. Mol. Biol. 15,* 220–231.
Kearns, D. R. (1976), *Prog. Nucleic Acid Res. Mol. Biol. 18,* 91–149.
Kearns, D. R., Lightfoot, D. R., Wong, K. L., Wong, Y. P., Reid, B. R., Cary, L., and Shulman, R. G. (1973a), *Ann. N.Y. Acad. Sci. 222,* 324–336.
Kearns, D. R., Patel, D., and Shulman, R. G. (1971a), *Nature (London) 229,* 338–340.
Kearns, D. R., Patel, D., Shulman, R. G., and Yamane, T. (1971b), *J. Mol. Biol. 61,* 265–270.
Kearns, D. R., and Shulman, R. G. (1974), *Acc. Chem. Res. 7,* 33.
Kearns, D. R., Wong, K. L., and Wong, Y. P. (1973b), *Proc. Natl. Acad. Sci. U.S.A. 70,* 3843–3846.
Kim, S. H., Sussman, J. L., Suddath, F. L., Quigley, G. J., McPherson, A., Wang, A. H. J., Seeman, N. C., and Rich, A. (1974), *Proc. Natl. Acad. Sci. U.S.A. 71,* 4970–4974.
Klug, A., Ladner, J., and Robertus, J. D. (1974), *J. Mol. Biol. 89,* 511–516.
Ladner, J. E., Jack, A., Robertus, J. D., Brown, R. S., Rhodes, D., Clark, B. F. C., and Klug, A. (1975), *Proc. Natl. Acad. Sci. U.S.A. 72,* 4414–4418.
Murao, K., Tanabe, T., Ishii, F., Namiki, M., and Nishimura, S. (1972), *Biochem. Biophys. Res. Commun. 47,* 1332–1337.
Nishimura, S. (1971), *Proced. Nucleic Acid Res. 2,* 542–564.
Olson, T., Fournier, M. J., Langley, K. H., and Ford, N. C. (1976), *J. Mol. Biol. 102,* 193–204.
Pearson, R. L., Weiss, J. F., and Kelmers, A. D. (1971), *Biochim. Biophys. Acta 228,* 770–774.
Quigley, G. J., Wang, A. H. J., Seeman, N. C., Suddath, F. L., Rich, A., Sussman, J. L., and Kim, S. H. (1975), *Proc. Natl. Acad. Sci. U.S.A. 72,* 4866–4870.
Reid, B. R. (1976), *Nature (London) 262,* 424–425.
Reid, B. R., Ribeiro, N. S., Gould, G., Robillard, G., Hilbers, C. W., and Shulman, R. G. (1975), *Proc. Natl. Acad. Sci. U.S.A. 72,* 2049–2053.
Reid, B. R., and Robillard, G. T. (1975), *Nature (London) 257,* 287–291.
Robillard, G. T., Tarr, C. E., Vosman, F., and Berendsen, H. J. C. (1976), *Nature (London) 262,* 363–369.
Schmidt, J., Buchardt, B., and Reid, B. R. (1970), *J. Biol. Chem. 245,* 5743–5750.
Schoemaker, H. J. P., and Schimmel, P. R. (1974), *J. Mol. Biol. 84,* 503–513.
Shulman, R. G., Hilbers, C. W., Wong, Y. P., Wong, K. L., Lightfoot, D. R., Reid, B. R., and Kearns, D. R. (1973), *Proc. Natl. Acad. Sci. U.S.A. 70,* 2042–2045.
Singer, C. E., and Smith, G. R. (1972), *J. Biol. Chem. 247,* 2989–3000.
Squires, C., and Carbon, J. (1971), *Nature (London), New Biol. 233,* 274–277.
Sussman, J. L., and Kim, S. H. (1976), *Science 192,* 853–858.
Wong, K. L., Bolton, P. H., and Kearns, D. R. (1975b), *Biochim. Biophys. Acta 383,* 446–451.
Wong, K. L., and Kearns, D. R. (1974), *Biopolymers 13,* 371–380.
Wong, K. L., Kearns, D. R., Wintermeyer, W., and Zachau, H. G. (1975a), *Biochim. Biophys. Acta 395,* 1–4.
Wong, K. L., Wong, Y. P., and Kearns, D. R. (1975c), *Biopolymers 14,* 749–762.